



## Design of a Quadruped Robot for Motion with Quasistatic Force Constraints

ELON RIMON\*

*Technion, Israel Institute of Technology, Department of Mechanical Engineering, Technion City,  
Haifa 32000, Israel*  
elon@robby.technion.ac.il

SHRAGA SHOVAL

*Industrial Engineering & Management, J&S Academic College, Ariel, Israel*

AMIR SHAPIRO

*Technion, Israel Institute of Technology, Department of Mechanical Engineering, Technion City,  
Haifa 32000, Israel*  
amirs@tx.technion.ac.il

**Abstract.** This paper presents a novel design of a four-legged “spider” robot capable of moving in a wide range of two-dimensional tunnels. The robot moves in a quasistatic manner, by stably bracing itself against the tunnel walls while moving its free parts to the next position. The design has been strongly influenced by the recent immobilization theory of Rimon and Burdick (1998a, 1998b). The theory dictates the minimum number of limbs such a mechanism can have, as well as the curvature of the mechanism footpads. The class of tunnel geometries dictates other key parameters of the robot, such as limb dimensions and number of degrees of freedom of each limb. We review the relevant components of the immobilization theory and describe its implications for the robot design. Then we describe our choice of other key design parameters of the robot. The spider-like robot will move under a worst-case assumption of slippery tunnel walls, and we also describe a locomotion strategy for the robot under this assumption. Finally, we describe an immobilization-based control algorithm for executing the motion strategy. The robot has been built, and experiments verifying its robustness with respect to leg-placement errors are described.

**Keywords:** stable locomotion, multi-legged robots, immobilization, robot design

### 1. Introduction

In conventional motion planning a wheeled mobile robot navigates toward a goal configuration while avoiding collision with obstacles. However, many motion planning problems are more suited for legged robots that interact with the environment in order to achieve stable locomotion. For example, surveillance

of collapsed structures for survivors, inspection and testing of complex pipe systems, and maintenance of hazardous structures such as nuclear reactors, all require motion in congested, unstructured, and complex environments. Furthermore, in such environments the robot cannot always rely on friction, as surfaces may be wet, oily, or icy. Our goal is to develop a general purpose multi-limbed mechanism that uses quasistatic motion to navigate in such environments. In *quasistatic motion*, inertial effects due to moving parts of the robot are kept small relative to the forces and torques of interaction

\*This research is supported by Grant 345/99 from the Israel Science Foundation.

between the robot and the environment. Motion is generated by reaction forces between the robot and the environment, and the planning of a path to the goal is subject to the constraint of maintaining stable equilibrium with the environment during the motion.

Spider-like and snake-like mechanisms are examples of robots that can move quasistatically in congested environments, and we now mention several works in these two areas. In previous work on spider-like mechanisms, researchers have taken one of the following two approaches. The first approach is exemplified by the pipe-crawling robots of Neubauer (1993, 1994), and Pfeiffer et al. (1996, 2000). In this approach a large number of simple limbs is used to stabilize the mechanism during locomotion. Additional degrees of freedom are sometime added to the central base to obtain the maneuverability necessary for moving in tunnel-like environments. The second approach is exemplified by the ladder-climbing robot of Dubowsky et al. (1992, 1999) and by the nuclear-reactor servicing robot of Stone et al. (1995). This approach seeks to design robots with a small number of limbs each having a relatively high degree of maneuverability. The central base in this approach is typically a simple rigid body. Each of the two approaches offers particular advantages, and researchers in this field seek to understand the consequences, in terms of system performance, of trading between the two approaches in any particular design.

In this paper we take the second design approach. Our main objective is to determine the smallest number of limbs a spider-like robot can have, and to design a viable mechanism having this number of limbs. The design should not only include details of mechanical structure, but also a motion paradigm for the spider and a control algorithm for executing the motion paradigm.

Before discussing snake-like mechanisms, we note that legged locomotion over a terrain is related to locomotion in congested environments. Examples of works in this area are by McGeer (1989), Hirose and Kunieda (1991), Boissonnat et al. (1992), Marhefka and Orin (1997), and Van-den-Doel and Pai (1997). However, we focus on locomotion in congested tunnel-like environments rather than legged locomotion over a terrain.

Snake-like mechanisms also interact with the environment during locomotion. They are related to spider-like mechanisms, since both mechanisms brace themselves against the environment while moving free parts toward a new position. Chrikjian and Burdick (1993) and Shan and Koren (1993) developed snake-like mechanisms that move by locking some of their links to the ground while allowing other links to move. These researchers, as well as Hirose and Morishima (1990), also investigated the use of motion patterns borrowed from biological snakes. However, all existing snake-like mechanisms interact with the environment via frictional contacts with the ground. In contrast, we focus on locomotion where a spider-like robot stably braces itself against a tunnel-like environment while moving its free parts. Moreover, the robot is required to operate under the assumption of slippery contacts (discussed below). Our problem is thus more akin to the way biological snakes move over smooth terrains (Gray, 1953). In such environments a snake propels itself by bracing against protrusions in the ground while moving free parts of its body in the forward direction.

Our goal is thus to design an autonomous spider-like robot capable of moving in a wide range of two-dimensional tunnels (Fig. 1). The mechanism is required to have the smallest number of limbs which still guarantee stable locomotion under the following

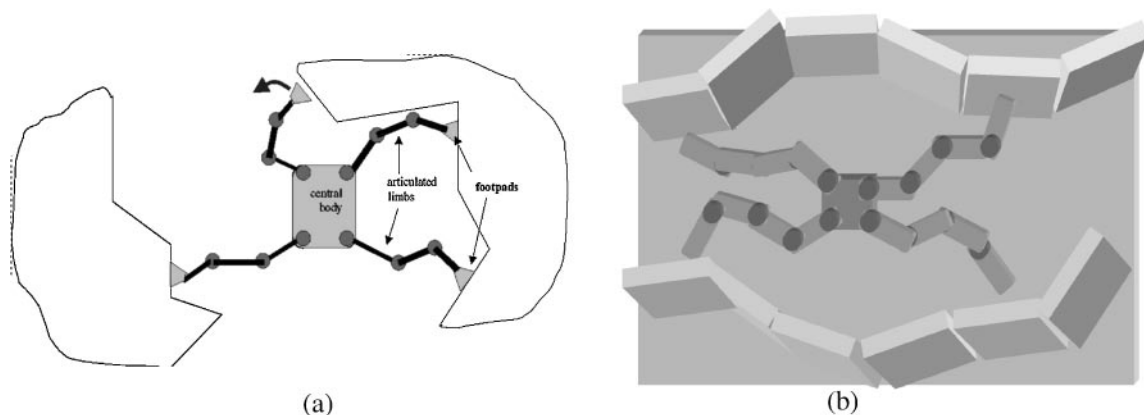


Figure 1. (a) A conceptual design, and (b) top view of a spider robot moving in a two-dimensional tunnel environment.

assumptions. First, we assume that each limb contacts the environment only through its distal link, called the *footpad*. The footpads have no suction cups and can only push against the environment. Second, we study locomotion in *two-dimensional horizontal tunnels with piecewise linear walls*. However, real tunnel walls may be wet, oily, or icy. Hence we assume *slippery tunnel walls*, so that locomotion must proceed without using friction. This restriction excludes tunnels of a particular simple geometry (such as two parallel lines), but most unstructured congested environments do have a complex geometry with many possible footholds within reach of the robot. Furthermore, since friction always acts to *enhance* the stability of a mechanism contacting the environment, a frictionless locomotion plan can also be executed in a frictional environment. Our last assumption is that the spider moves *quasistatically*, by stably bracing itself against the tunnel walls while changing its internal configuration to allow motion of its free parts to the next position. This approach enables the robot to reliably operate even when unpredicted external forces are applied, such as drag forces from surrounding air or liquids, unexpected collisions, or uneven loads.

The paper is organized as follows. We first review the relevant components of the immobilization theory of Rimon and Burdick (1998a, 1998b). Then we describe how the theory dictates the smallest number of limbs a spider-like mechanism can have, as well as the curvature of the footpads required for stability. The class of tunnel geometries dictates other key parameters of the robot, such as limb dimensions and number of degrees of freedom of each limb. We describe these design considerations, accounting for issues such as the number of degrees of freedom, dimensions, and mechanical struc-

ture of various parts of the spider robot. Next we describe a locomotion strategy for the spider under the assumption of slippery tunnel walls. Then we describe a control algorithm for executing the motion strategy by exploiting the immobilization forces applied by the tunnel walls on the spider. The spider has been built, and we describe preliminary locomotion experiments that verify the mechanism's robustness with respect to footpad placement errors. The paper concludes with a discussion of future extension to locomotion in non-horizontal and frictional tunnel environments.

## 2. C-Space Approach to Rigid Body Mobility

In this section we describe the essential components of the immobilization theory developed by Rimon and Burdick (1998a, 1998b), then draw conclusions pertaining to the mechanical structure of the spider robot. This theory is concerned with the mobility of a rigid object  $\mathcal{B}$  held by  $k$  stationary and *frictionless* finger bodies  $\mathcal{A}_1, \dots, \mathcal{A}_k$  in an equilibrium grasp. The same analysis holds for a  $k$ -limbed mechanism bracing against an environment in a static equilibrium posture. If we momentarily "freeze" the joints of the mechanism, the mechanism plays the role of the object  $\mathcal{B}$ , while the tunnel walls play the role of the stationary bodies  $\mathcal{A}_1, \dots, \mathcal{A}_k$ . The mobility analysis of  $\mathcal{B}$  focuses on its configuration space (*c-space*). For planar bodies this configuration space is parametrized by  $q = (d_x, d_y, \theta) \in \mathbb{R}^3$ . The fingers or tunnel walls are represented in the configuration space of  $\mathcal{B}$  as *c-space obstacles* (*c-obstacles*). As shown in Fig. 2, the *c-obstacle* due to a stationary body  $\mathcal{A}_i$  is the set of all configurations where  $\mathcal{B}$  intersects the stationary  $\mathcal{A}_i$ . Thus, if  $q_0$  is  $\mathcal{B}$ 's contact configuration

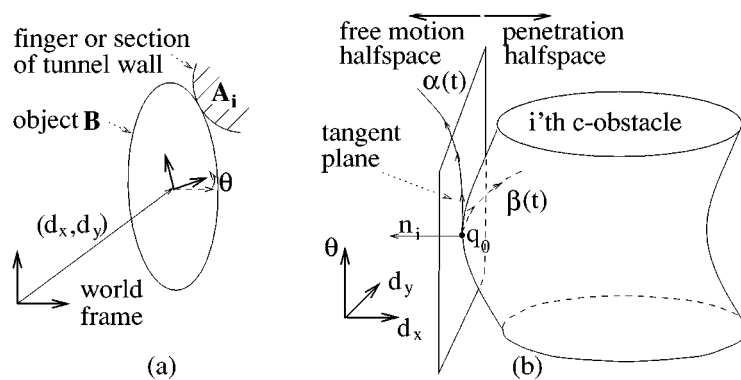


Figure 2. The first-order approximation to the free motions of  $\mathcal{B}$  at  $q_0$ .  $\dot{\alpha}(0)$  and  $\dot{\beta}(0)$  are 1st order roll-slide motions.  $\alpha(t)$  locally lies in freespace,  $\beta(t)$  locally penetrates the *c-obstacle*.

with  $\mathcal{A}_i$ ,  $q_0$  lies on the c-obstacle boundary, denoted  $\mathcal{S}_i$ . When  $\mathcal{B}$  is contacted by  $k$  bodies,  $q_0$  lies on the intersection of  $\mathcal{S}_i$  for  $i = 1, \dots, k$ . We denote tangent vectors in c-space by  $\dot{q}$ , and use the notation  $T_q \mathbb{R}^3$  and  $T_q \mathcal{S}_i$  for the tangent space of  $\mathbb{R}^3$  and  $\mathcal{S}_i$  at  $q$ .

### 2.1. 1st and 2nd Order Free Motions

The mobility of  $\mathcal{B}$  relative to the bodies  $\mathcal{A}_1, \dots, \mathcal{A}_k$  is characterized by the following notion of free motions. By definition, the *free motions* of  $\mathcal{B}$  are those local motions of  $\mathcal{B}$  along which it either breaks away from or maintains surface contact with the bodies  $\mathcal{A}_1, \dots, \mathcal{A}_k$ . In c-space, the free motions of  $\mathcal{B}$  at  $q_0$  are the c-space paths that emanate from  $q_0$  and locally lie in the *free c-space*, which is the complement of the c-obstacle interiors. The first-order geometry of the free paths and the c-obstacle boundaries determines what we term the *first-order mobility* of  $\mathcal{B}$  at  $q_0$ . Formalizing this notion, let  $n_i(q_0)$  be the outward pointing unit normal to  $\mathcal{S}_i$  at  $q_0$  (Fig. 2(b)). Then the 1st order free motions of  $\mathcal{B}$  at  $q_0$  is the set (halfspace of  $T_{q_0} \mathbb{R}^3$ ) of tangent vectors  $\dot{q}$  satisfying:

$$M_i^1(q_0) \triangleq \{\dot{q} \in T_{q_0} \mathbb{R}^3 : n_i(q_0) \cdot \dot{q} \geq 0\}.$$

Tangent vectors  $\dot{q} \in T_{q_0} \mathbb{R}^3$  satisfying  $n_i(q_0) \cdot \dot{q} = 0$  are called 1st order roll-slide motions, while the other tangent vectors in  $M_i^1(q_0)$  are called 1st order escape motions. For  $k$  fingers or tunnel walls, the set of 1st order free motions is:  $M_{1,\dots,k}^1(q_0) \triangleq \bigcap_{i=1}^k M_i^1(q_0)$ .

In other words, along 1st order escape motions  $\mathcal{B}$  increases its distance from  $\mathcal{A}_i$  to first-order, which implies that it locally breaks away from  $\mathcal{A}_i$ . Along 1st order roll-slide motions  $\mathcal{B}$  maintains surface contact with  $\mathcal{A}_i$  to first-order, and *it is not possible* to determine from first-order considerations if  $\mathcal{B}$  locally breaks away or penetrates  $\mathcal{A}_i$ . For example, the c-space curves  $\alpha(t)$  and  $\beta(t)$  in Fig. 2 have the same tangent vector at  $q_0$ , and thus are equivalent to first-order. Yet  $\alpha(t)$  locally lies in the free c-space, while  $\beta(t)$  locally penetrates the c-obstacle. As we shall see, *all the free motions of  $\mathcal{B}$  at a frictionless equilibrium grasp or posture are necessarily roll-slide to first-order*. Thus, in order to fully characterize the mobility of  $\mathcal{B}$  at an equilibrium grasp or posture, the second-order properties of its local motions must be considered. This insight, and the ensuing 2nd order index, are a major new tool which is employed in the design of the spider robot.

The second-order geometry of the free-motion curves and the c-obstacle boundaries is determined by their curvature and curvature form, respectively. The *curvature form*, describing the curvature of  $\mathcal{S}_i$  at  $q_0 \in \mathcal{S}_i$ , is given by the quadratic form  $\kappa_i(q_0, \dot{q}) \triangleq \dot{q}^T Dn_i(q_0) \dot{q}$ , where  $\dot{q} \in T_{q_0} \mathcal{S}_i$  and  $Dn_i$  is the derivative of the unit normal  $n_i$ . Ref. Rimon and Burdick (1998a) contains a formula for  $\kappa_i(q_0, \dot{q})$  in terms of the surface normals and curvatures of the contacting bodies. The free-motion curves are determined to second-order by their *velocity and acceleration* at  $q_0$ , as follows. The 2nd order free motions of  $\mathcal{B}$  at  $q_0$  is the subset of  $(\dot{q}, \ddot{q})$  satisfying:

$$M_i^2(q_0) \triangleq \{(\dot{q}, \ddot{q}) : n_i(q_0) \cdot \dot{q} = 0 \quad \text{and} \\ \dot{q}^T [Dn_i(q_0)] \dot{q} + n_i(q_0) \cdot \ddot{q} \geq 0\}.$$

Analogous to the first-order case, pairs  $(\dot{q}, \ddot{q})$  that satisfy  $n_i(q_0) \cdot \dot{q} = 0$  and  $\dot{q}^T [Dn_i(q_0)] \dot{q} + n_i(q_0) \cdot \ddot{q} = 0$  are called 2nd order roll-slide motions, while the other pairs in  $M_i^2(q_0)$  are called 2nd order escape motions. Note that the definition of 2nd order free motions focuses on those curves which are 1st order roll-slide motions. It is important to stress again that 1st order roll-slide motions are the only motions available for  $\mathcal{B}$  when it is held in an equilibrium grasp or posture. Thus, if all the 1st order roll-slide motions of  $\mathcal{B}$  are 2nd order penetration motions,  $\mathcal{B}$  is completely immobilized at the equilibrium.

### 2.2. 1st and 2nd Order Mobility Indices

We say that  $\mathcal{B}$  is *completely immobile* if its configuration  $q_0$  is completely isolated from the free c-space by the c-obstacles associated with the bodies  $\mathcal{A}_1, \dots, \mathcal{A}_k$ . Physically, this means that all the local c-space motions of  $\mathcal{B}$  which start at  $q_0$  cause the object to penetrate the bodies  $\mathcal{A}_1, \dots, \mathcal{A}_k$ . We now describe mobility indices which are useful for quantifying the amount of free-motions available to  $\mathcal{B}$  at an equilibrium. The *mobility indices* are coordinate invariant integer-valued functions that measure the instantaneous mobility of  $\mathcal{B}$  when it is held in a frictionless equilibrium grasp or posture by  $k$  bodies  $\mathcal{A}_1, \dots, \mathcal{A}_k$ . At an equilibrium the net wrench (force and torque) generated by the contact forces is zero. It can be verified that the wrench generated by a contact force which acts along the  $i$ th contact normal is a positive multiple<sup>1</sup> of the c-obstacle normal  $n_i(q_0)$ . An *equilibrium grasp or posture* is

therefore characterized by the condition that zero lies in the convex hull of  $n_1(q_0), \dots, n_k(q_0)$ . That is, there exist scalars  $\lambda_1, \dots, \lambda_k$  such that

$$\lambda_1 n_1(q_0) + \dots + \lambda_k n_k(q_0) = \vec{0}, \quad (1)$$

where  $\lambda_i \geq 0$  and  $\sum_{i=1}^k \lambda_i = 1$ .

At a  $k$ -contact equilibrium grasp or posture, the intersection of the 1st order free motion halfspaces associated with the individual contacts,  $M_{1,\dots,k}^1(q_0) = \bigcap_{i=1}^k M_i^1(q_0)$ , forms a subspace. This subspace is the set of instantaneous motions which are simultaneously 1st order free with respect to each of the bodies  $\mathcal{A}_1, \dots, \mathcal{A}_k$ . The 1st order mobility index of an equilibrium grasp or posture is defined as the dimension of the subspace  $M_{1,\dots,k}^1(q_0)$ . The index is denoted  $m_{q_0}^1$ , and for non-redundant grasps  $m_{q_0}^1 = \max\{0, 4-k\}$  where  $k$  is the number of contacts. Immobilization of  $\mathcal{B}$  by first-order effects is achieved when the 1st order mobility index vanishes. Thus at least  $k=4$  contacts are required for first-order immobilization. It follows that a legged mechanism moving in a frictionless two-dimensional environment requires at least *five* limbs, as one limb must always be free to move to a new position.

However, it is possible to further reduce the number of limbs by considering second-order (or curvature) effects at the contacts. The 2nd order mobility index for a  $k$ -contact equilibrium grasp or posture is based on the c-space curvature form of  $\mathcal{S}_i$ ,  $\kappa_i(q_0, \dot{q})$ . Consider the coefficients  $\lambda_i$  in the equilibrium condition (1). It is shown in Rimon and Burdick (1998b) that the weighted sum of the c-obstacle curvatures, called the *relative c-space curvature*, has a coordinate invariant structure which is related to the second-order mobility of  $\mathcal{B}$  at the equilibrium. These notions are made precise in the following definition.

**Definition 1.** Let  $\lambda_1, \dots, \lambda_k$  be the coefficients in the  $k$ -contact equilibrium equation (1). Let the **c-space relative curvature form** of the equilibrium be the quadratic form:

$$\kappa_{\text{rel}}(q_0, \dot{q}) = \sum_{i=1}^k \lambda_i \kappa_i(q_0, \dot{q})$$

such that  $\dot{q} \in M_{1,\dots,k}^1(q_0)$ .

Then the **2nd order mobility index** of the equilibrium, denoted  $m_{q_0}^2$ , is the **number of non-negative eigenvalues** of the matrix of the c-space relative curvature  $\kappa_{\text{rel}}(q_0, \dot{q})$ .

By definition,  $m_{q_0}^1$  is an upper bound on the possible values of  $m_{q_0}^2$  i.e.,  $0 \leq m_{q_0}^2 \leq m_{q_0}^1$ . Hence *second-order (or curvature) effects always act to reduce the mobility of  $\mathcal{B}$* . We say that  $\mathcal{B}$  is *immobile to second-order* when  $m_{q_0}^2 = 0$ . For  $k \geq 4$  contacts  $m_{q_0}^1 = 0$ , and  $\mathcal{B}$  is completely immobile to first-order. However, if we wish to reduce the number of contacts, we must use second-order effects. In other words, by suitable choice of curvature at the contacts, it is possible to immobilize  $\mathcal{B}$  using only  $k=2, 3$  contacts. In these cases  $\mathcal{B}$  is not immobile to first-order ( $m_{q_0}^1 > 0$ ), but may be immobile to second-order ( $m_{q_0}^2 = 0$ ).

### 2.3. Graphical Depiction of the Free Motions

We wish to determine suitable footpads curvature that would guarantee second-order immobilization of the mechanism using only *three* contacts with the environment. To do this, we first present a graphical technique for rendering the 1st and 2nd order free motions. The 1st order roll-slide motions correspond to tangent vectors in  $T_{q_0}\mathcal{S}_i$ . For planar bodies, these motions admit the parametrization depicted in Fig. 3(a). Let  $l_i$  denote the line of the contact normal between  $\mathcal{A}_i$  and  $\mathcal{B}$ . Let  $\rho_i$  be the distance along  $l_i$  from the  $i$ th contact point, such that  $\rho_i$  is positive on  $\mathcal{B}$ 's side of the contact and negative on  $\mathcal{A}_i$ 's side. Then the tangent vectors in  $T_{q_0}\mathcal{S}_i$  correspond to instantaneous rotations of  $\mathcal{B}$  about points on the line  $l_i$  at a distance  $\rho_i$ , as  $\rho_i$  sweeps  $l_i$  from  $-\infty$  to  $\infty$ . Note that  $\rho_i$  is allowed to attain values in  $\mathbb{R} \cup \{\infty\}$ , with the interpretation that rotation about an axis "at infinity" gives pure translation in a direction perpendicular to  $l_i$ . Thus, for planar bodies we can parametrize the tangent plane  $T_{q_0}\mathcal{S}_i$  by the parameters  $\rho_i$  and  $\omega$ , where  $\omega$  is the angular velocity about an axis located at a distance  $\rho_i$  on  $l_i$ .

Next we describe a graphical partition of the line  $l_i$  into 2nd order free and 2nd order penetration motions (Fig. 3(b)). Let  $r_{\mathcal{A}_i}$  and  $r_{\mathcal{B}_i}$  be the radii of curvature of  $\mathcal{A}_i$  and  $\mathcal{B}$  at the contact point. It is shown in Ref. (Rimon and Burdick, 1998a) that the curvature form  $\kappa_i(q, \dot{q})$  can be written for  $\dot{q} = (0, \omega)$  as:

$$\kappa_i(q, (0, \omega)) = \frac{1}{r_{\mathcal{A}_i} + r_{\mathcal{B}_i}} (\rho_i - r_{\mathcal{B}_i})(\rho_i + r_{\mathcal{A}_i}) \omega^2, \quad (2)$$

where  $\dot{q} = (0, \omega)$  represents instantaneous rotation of  $\mathcal{B}$  about a point at a distance  $\rho_i$  along  $l_i$ . Since the tangent space  $T_q\mathcal{S}_i$  corresponds to these instantaneous rotations, the sign of  $\kappa_i(q, \dot{q})$  for all  $\dot{q} \in T_q\mathcal{S}_i$  can be determined by evaluating (2) for  $-\infty \leq \rho_i \leq \infty$ . For

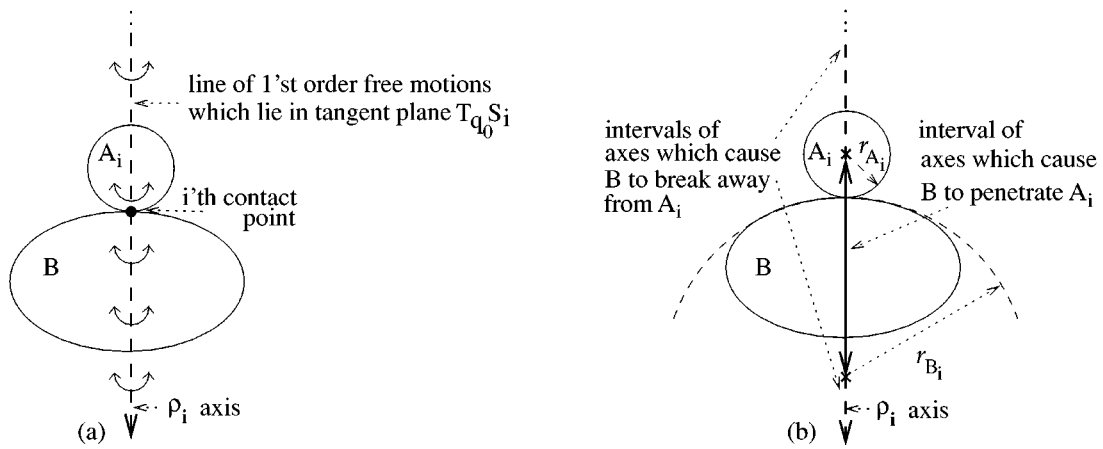


Figure 3. Graphical depiction of (a) the 1st order roll-slide motions, and (b) the 2nd order motions of  $B$  with respect to  $A_i$ .

example, if  $B$  and  $A_i$  are convex at the contact point, then  $r_{B_i} > 0$  and  $r_{A_i} > 0$ . In this case the curvature  $\kappa_i$  is negative for  $\rho_i$  in the interval  $-r_{A_i} < \rho_i < r_{B_i}$ , and positive in the intervals  $\rho_i < -r_{A_i}$  and  $\rho_i > r_{B_i}$ . If one of the bodies,  $B$  say, is concave at the contact point, then  $r_{B_i} < 0$  and the curvature is negative in the interval  $-|r_{B_i}| \leq \rho_i \leq -r_{A_i}$ .

2.4. Implications for the Spider's Design

We now discuss some implications of the immobilization theory to the spider's structure. The 1st and 2nd order mobility indices allow immobilization which is based on surface curvature in addition to the more conventional reliance on contact normals. Based on conventional first-order considerations, it was previously thought that *four* frictionless contacts are required to immobilize generic 2D objects (Markenscoff et al.,

1990; Reuleaux, 1963). However, Czyzowicz et al. (1991) and Rimon and Burdick (1995) have recently shown that generic 2D objects can be immobilized by only *three* frictionless fingers with convex shape, provided that the fingers are sufficiently flat at the contacts. Equivalently, *any multi-limbed mechanism can immobilize itself in a frictionless two-dimensional environment using only three limbs with sufficiently flat convex footpads*. The spider must therefore have at least *four* limbs—three limbs for immobilization and at least one additional limb for establishing a new foothold during locomotion. In our prototype, we have chosen to use the minimum number of four limbs for the spider.

Let us consider the proper choice of footpad curvature. In a 3-legged equilibrium, the contact-force lines must intersect at a common point  $p$  (Fig. 4). The set of 1st order roll-slide motions available to the mechanism is a one-dimensional subspace (since  $m_{q_0}^1 = 1$ ),

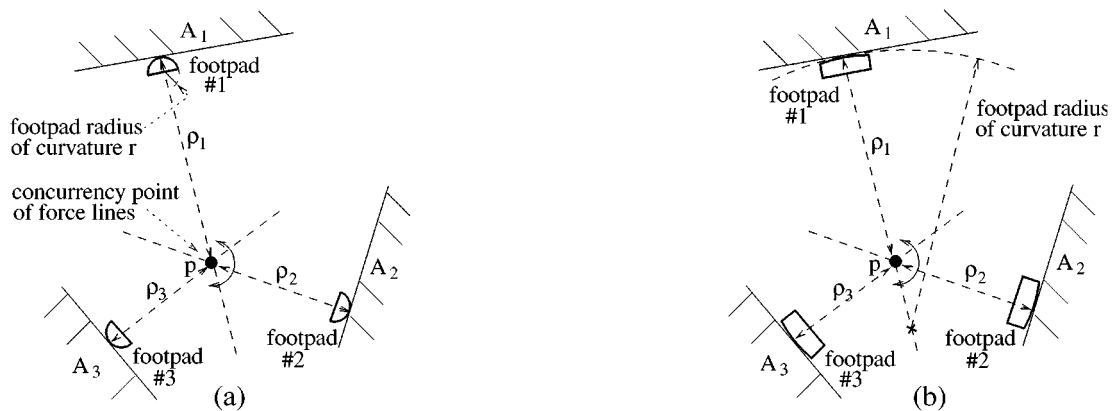


Figure 4. (a) The spider is not immobile since  $r < \rho_i$ . (b) The spider is immobile since the footpads satisfy  $r > \rho_i$  for  $i = 1, 2, 3$ .

consisting of instantaneous rotations of the mechanism about  $p$ . (That is, instantaneous rotations of the mechanism as a single rigid body.) For complete immobility we must have  $m_{q_0}^2 = 0$ . This condition can be interpreted as the requirement that the footpads be sufficiently flat at the contacts, as to prevent instantaneous rotations of the mechanism about  $p$ . A sufficient condition for  $m_{q_0}^2 = 0$  is that *the radius of curvature of the  $i$ th footpad be larger than the distance between the  $i$ th contact point and the concurrency point  $p$ , for  $i = 1, 2, 3$* . In this case the c-space curvature of each contact satisfies  $\kappa_i < 0$  for instantaneous rotations about  $p$  (Eq. (2)), and  $\kappa_{\text{rel}} = \sum_{i=1}^3 \lambda_i \kappa_i < 0$ . Consequently  $m_{q_0}^2 = 0$  and the mechanism is completely immobilized by the tunnel walls. The footpads in Fig. 4 have a radius of curvature  $r$ , and the distance between the  $i$ th contact and  $p$  is  $\rho_i$ . When  $r < \rho_i$  the spider is *not* immobile, since in this case rotation of the mechanism about  $p$  is 2nd order free for each of the contacts (Fig. 4(a)). When the footpads' radius-of-curvature is larger than the tunnel's width, the sufficient condition holds true and the mechanism is completely immobilized (Fig. 4(b)).

In general, for any given tunnel geometry there exists an upper bound on the footpads' curvature which guarantees immobilization of the mechanism in every 3-legged posture in the tunnel (Rimon et al., 1999). This bound depends on the maximal distance of the point  $p$  from the contacts in the given tunnel, and it increases as the tunnel-segments become parallel to the tunnel's central axis. In our design, we have selected the footpads' radius-of-curvature to be 1.5 times the tunnel's average width. This choice guarantees immobilization of all 3-legged postures whose intersection point  $p$  lies at a distance of tunnel-width away from the tunnel's central axis.

Finally, we note that the lower bound of three limbs is a tight lower bound, for the following reasons. If one wishes to use only two limbs, one must either use friction or exploit concavities in the environment. However, our focus is on locomotion which makes no use of frictional effects. As for exploiting concavities, we assume piecewise-linear tunnel walls, and these walls form concavities only at particular corners. Rather than seek these relatively rare localities, we assume that the limbs contact the environment anywhere along the linear (hence convex) tunnel walls. However, there are well known examples in the grasping literature (Rimon and Burdick, 1995) of objects which cannot be immobilized with only two frictionless convex fingers.

In our case, this means that *three* limbs must be used in order to guarantee immobilization of the spider in arbitrary tunnel environments.

### 3. Spider Robot Design Considerations

Thus far we have established that the spider will have four limbs, with the footpads' curvature sufficiently flat as to guarantee immobilization. In this section we describe the considerations that have led us to choose other key design parameters of the spider. First we consider kinematic parameters—the number of degrees of freedom and the dimensions of the spider. Then we consider the mechanical structure of the spider's limbs and footpads.

#### 3.1. The Number of Degrees of Freedom

As discussed below, the spider alternates between two modes of locomotion. In the first mode, called *limb lifting*, the spider braces itself against the environment with three limbs and lifts its fourth limb to a new position. In the second mode, called *limb repositioning*, the spider contacts the environment with all four limbs while repositioning its contacts with the environment as to allow lifting of a new limb. See Section 4 for more details.

We now discuss our choice of the number of degrees of freedom for each limb of the spider. First consider the limb-repositioning mode of locomotion. We wish to allow arbitrary placement of the central body in the plane (position and orientation) during this mode of locomotion. The closed-loop mechanism formed by the spider bracing against the environment should have at least three degrees of freedom. Moreover, we wish to attain this degree of mobility when the four footpads of the spider are stationary with respect to the environment. (For clarity, we note that each limb has a single footpad which forms the distal link of the limb.) In general, the number of degrees of freedom of a planar mechanism consisting of #link links and #joint joints is:

$$\# \text{d.o.f.} = 3(\# \text{link} - 1_{\text{environment}}) - 2\# \text{joint}, \quad (3)$$

where the number of links includes a stationary link representing the environment. Let  $n_{\text{limb}}$  be the number of links in each limb. Since each limb is a serial chain, there are  $n_{\text{limb}}$  joints in each limb, and consequently  $\# \text{joint} = 4n_{\text{limb}}$ . The spider has four limbs, and the

distal link of each limb (the footpad) remains stationary. Hence  $\#link = 4n_{limb} + 1_{central-body} + 1_{environment} - 4_{footpads}$ . Substituting these values in (3) gives:

$$\begin{aligned} \# \text{d.o.f.} &= 3(4n_{limb} + 1_{central-body} - 4_{footpads}) - 8n_{limb} \\ &= 4n_{limb} - 9. \end{aligned}$$

The requirement  $\# \text{d.o.f.} = 4n_{limb} - 9 \geq 3$  implies that  $n_{limb} \geq 3$ . Thus *three* links and *three* joints for each limb would suffice during limb repositioning. Consider now the limb-lifting mode of locomotion. We may assume that the central-body makes only local motions during this mode of locomotion. The free limb therefore has an essentially fixed base while it attempts to reach a new foothold position. In principal the limb's three degrees of freedom should suffice to arbitrarily place its footpad in the plane (position and orientation). However, when operating in a congested environment, additional degrees of freedom are required in order to accommodate obstacles. But motion planning and control become substantially more complex as the number of degrees of freedom increases. (Especially since the total number of degrees-of-freedom increases by increments of four.) Thus, in order to increase maneuverability while retaining a manageable mechanism complexity, we add *one* additional link and joint to each limb, resulting in *four* links and *four* joints for each limb.

### 3.2. The Spider's Dimensions

We now describe our choice of two key dimensions of the spider robot. The central body of the spider is made of a thick square plate, and the first parameter is the width, denoted  $b$ , of the central body. The second parameter is the total length, denoted  $l$ , of each limb. (The dimension of the individual links is determined below.) The ratio  $l/b$  is related to the desired maneuverability of the spider as follows. Let  $D_{min}$  and  $D_{max}$  be the minimal and maximal widths of the tunnel. Then  $b$  must be smaller than  $D_{min}$  to allow motion of the central body through the tunnel, while the quantity  $b + 2l$  must be larger than  $D_{max}$  to allow the spider to reach both sides of the tunnel. Assuming that  $D_{min} = b$  and  $D_{max} = b + 2l$ , we define the *maneuverability index* as the ratio:

$$M = \frac{D_{max}}{D_{min}} = 1 + 2\frac{l}{b}. \quad (4)$$

A large maneuverability index is more desirable, since it reflects an increased ability of the spider to move in a given tunnel environment. In our design, we have assumed tunnels with a maneuverability index of  $M = 10$ , which gives the ratio  $l/b \cong 5$ . However, while a large  $M$  increases the spider's maneuverability, it causes an undesirable overlap between the limbs' reachable areas. This concern is addressed by the spider's mechanical structure discussed below.

Next we focus on the spider's *radius of reachability*, defined as  $R = l + b/2$ . This radius represents the distance from the center of the central body to the end of a completely stretched limb. The choice of  $R$  influences the ability of the robot to reach desired footholds along the tunnel walls. To understand this influence, consider a particular triplet of tunnel segments, denoted  $I_{i_1}, I_{i_2}, I_{i_3}$ . (The tunnel, recall, has piecewise linear walls.) At a 3-legged equilibrium posture the contact-force lines intersect at a common point  $p$ . The collection of points  $p$  corresponding to all possible equilibrium footholds on  $I_{i_1}, I_{i_2}, I_{i_3}$  is a polygonal region denoted  $P_{i_1, i_2, i_3}$  (Fig. 5(a)). For frictionless contacts  $P_{i_1, i_2, i_3}$  is simply the intersection of the strips perpendicular to the segments  $I_{i_1}, I_{i_2}, I_{i_3}$ . The collection of all polygons  $P_{i_1, i_2, i_3}$ , where  $i_1, i_2, i_3$  range over the tunnel segments, describes all possible 3-legged equilibrium postures in a given tunnel.<sup>2</sup>

Next we impose a reachability constraint on the polygons  $P_{i_1, i_2, i_3}$ . Figure 6 shows a randomly selected piecewise-linear tunnel whose average width is one unit. For each triplet  $I_{i_1}, I_{i_2}, I_{i_3}$  of tunnel segments, we first determine the corresponding equilibria polygon  $P_{i_1, i_2, i_3}$ . Then we discretize  $P_{i_1, i_2, i_3}$ , and for each point  $p \in P_{i_1, i_2, i_3}$  perform the following two steps. First we determine the location of the footholds corresponding to  $p$  on the tunnel segments  $I_{i_1}, I_{i_2}, I_{i_3}$ . Then we plot the region formed by intersecting three discs of radius  $R$  (the robot's radius), centered at the three footholds (Fig. 5). The resulting *reachability region* represents all central-body locations from which triplets of equilibrium footholds on the segments  $I_{i_1}, I_{i_2}, I_{i_3}$  can be reached. Figure 6 shows the resulting reachability regions for several robot diameters. To allow a continuous motion of the central body,  $R$  should be chosen such that the reachability regions form a contiguous area along the tunnel. As the figure shows, a robot diameter of  $2R = 1.15$  units already provides ample overlap of the reachability regions. In our experiment the tunnel's average width is 1.1 meters, and we selected the spider's diameter as  $2R = 1.3$  meters. Combining the equations

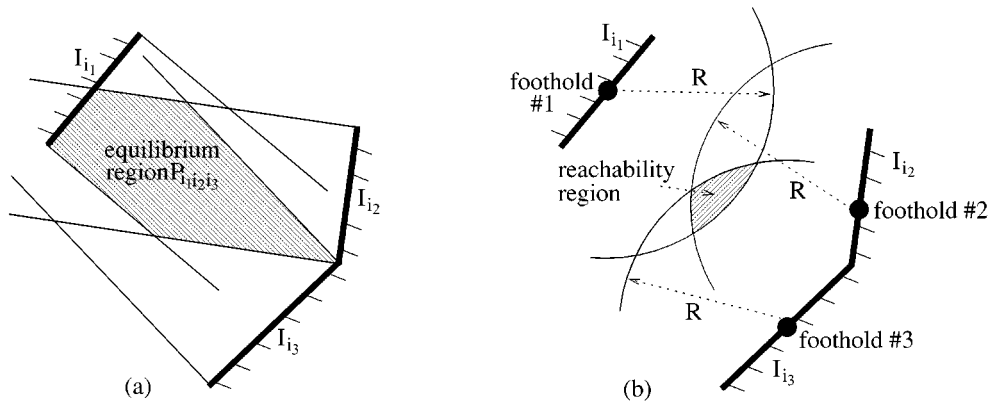


Figure 5. (a) The equilibrium region formed by intersecting three vertical strips. (b) The reachability region corresponding to a particular triplet of footholds.

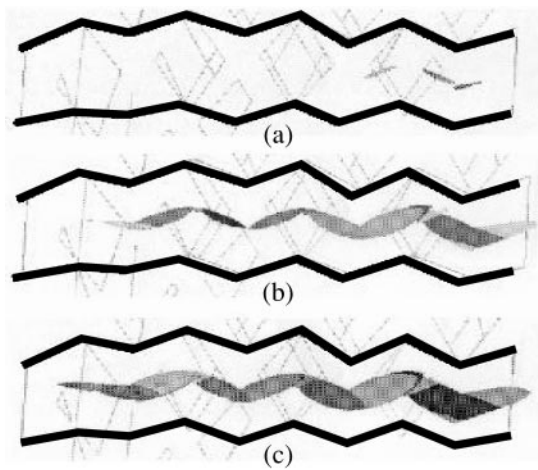


Figure 6. Reachability regions corresponding to a unit-width tunnel. (a)  $2R = 0.85$  units, (b)  $2R = 1.05$  units, (c)  $2R = 1.15$  units.

$2R = 2l + b = 1.3$  with  $l/b = 5$ , the limbs' length is  $l = 60$  cm and the central-body's size is  $b = 12$  cm.

### 3.3. Limbs Mechanical Design

First we describe how the limbs are attached to the central body. To minimize inter-link interference, we designed two types of limbs—an upper and a lower limb. In an upper limb all driving mechanisms are positioned upward, above the plane of the central body. In a lower limb all driving mechanisms are positioned downward, underneath the central body. To minimize inter-link interference, the spider has two upper limbs and two lower limbs. As Fig. 7(a) shows, the upper limbs never interfere with the lower limbs (except for a possible interference of the passive supports, discussed below). Furthermore, to minimize interference

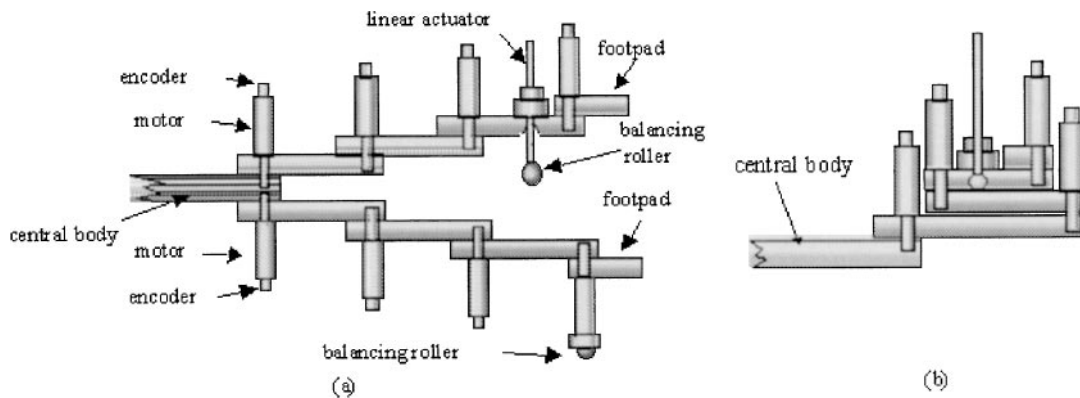


Figure 7. (a) Schematic description of the upper and lower limbs. (b) An upper limb in its retracted configuration.

between the two upper (lower) limbs, these limbs are attached at diagonally opposite corners of the central body. The resulting design allows simultaneous motion of the four limbs with minimal inter-link interference.

Next we describe the spider's weight supports. Recall that the spider moves in a horizontal two-dimensional tunnel by pushing against the tunnel walls. However, gravitational forces in the direction normal to the horizontal plane may generate a torque that can tip the robot out of the horizontal plane. The spider's weight must therefore be supported in a way which would prevent its tilting during locomotion. Figure 7(a) shows the two types of supporting mechanisms attached to the robot. The first mechanism is a balancing roller-ball attached underneath the central body and the third link of the lower limbs. The second mechanism is a linearly actuated roller-pad support, attached underneath the third link of the upper limbs. The latter support is actuated as to allow its lifting when an upper limb passes over a lower limb. The resulting arrangement of five supports provides ample balancing of the spider against any gravitational tilting.

To achieve maximum motion flexibility of each limb, we selected the links' length in a *decreasing* order. The link closest to the central body is 24 cm long, and the next ones have lengths of 18 cm, 14 cm, and 4 cm. These lengths allow each limb to completely retract into its first link, allowing the robot to maneuver itself in congested environments and through narrow passageways. Figure 7(b) shows an upper limb in its retracted configuration. Note that the balancing roller-pad is lifted into a special cavity, so that it would not interfere with the motion of the links. Finally, each link is designed to have an adjustable length, allowing

a screw-adjustable variation of 33% in the length of each link.

### 3.4. Footpad Mechanical Design

The distal links of the limbs, or footpads, are the only parts of the robot that contact the environment. As discussed above, the footpads curvature must be sufficiently flat to guarantee immobilization of the spider during 3-legged bracing. Since the tunnel walls are assumed piecewise linear, perfectly flat footpads would give the best immobilization. However, we wish to avoid the overhead incurred by controlling the placement of such footpads. We therefore designed two types of footpads which are easier to control. The first footpad design, shown in Fig. 8(a), is a single body curved with a large radius-of-curvature that guarantees immobilization. The curved footpads can easily establish a point-contact with the environment, and by controlling the location of these contacts with the environment we can establish immobile equilibrium postures.

The second footpad design simulates a flat footpad (which gives maximal immobilization), while avoiding the overhead involved in placing a flat footpad on a flat surface. This footpad also reduces the contact friction to almost zero, allowing validation of the spider's locomotion in a truly slippery environment. As Fig. 8(b) shows, the footpad mechanism consists of a rotating triangular flange with two roller-bearings at each edge, and an electromagnetic clutch that controls the flange's rotation axis. When the footpad reaches a contact surface, the clutch is released and one of the flange's edges passively adjusts itself to the contact surface. When contact is established, the clutch is activated

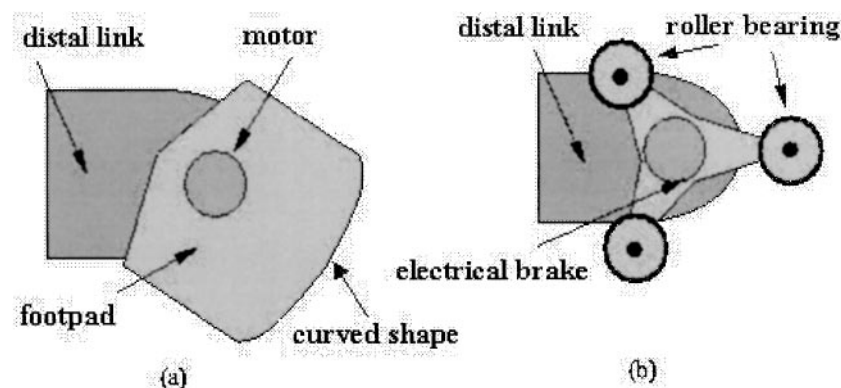


Figure 8. Two footpad designs. (a) A geometric curvature design. (b) A frictionless contact design.

and the footpad becomes a rigid body with two roller-bearings in contact with the environment. The bearings allow only perpendicular forces to be transferred at the contacts, thereby emulating a truly slippery environment. It is worth mentioning that Nagakubo and Hirose (1994) employed similar footpads in their design of a quadruped wall-climbing robot.

#### 4. The Spider Robot Motion

We now describe a motion paradigm that allows quasistatic locomotion of the spider in a slippery tunnel environment. The motion consists of two phases which repeat until the spider reaches its goal. In the first phase, called *limb lifting*, the spider braces against the environment with three limbs while the fourth limb moves toward a new foothold position. During this motion the central base and the three limbs contacting the environment move in a way which keeps the contacting footpads stationary with respect to the environment. At the end of a limb-lifting phase all four limbs contact the environment. However, before the spider can lift a new limb, it must ensure that the remaining three limbs form an equilibrium posture. For clarity, let the limbs be denoted  $L_1, L_2, L_3, L_4$ . Suppose that the spider initially lifts the limb  $L_1$ , while the limbs  $L_2, L_3, L_4$  maintain a 3-legged equilibrium posture (Fig. 9(a)). To be able to lift a new limb, say  $L_4$ , the spider must first ensure that the force-lines of the limbs  $L_1, L_2, L_3$  intersect at a common point. However, the limbs  $L_2$  and  $L_3$  are common to both limb-triplets, and the force-lines of  $L_2$  and  $L_3$  intersect at a unique point. Hence we must first move the location of the contact points of the limbs  $L_2$  and  $L_3$  with the tunnel walls before the limb  $L_4$  can be lifted.

In the second phase, called *limb repositioning*, the spider slides two limbs along the tunnel walls, while

the other two limbs maintain a fixed contact with the environment. For example, in Fig. 9(b) the spider slides the limbs  $L_2$  and  $L_3$  along the tunnel walls, while the limbs  $L_1$  and  $L_4$  maintain a fixed contact with the environment. During this sliding, the intersection point of the force-lines of the limbs  $L_2$  and  $L_3$  moves forward, until it reaches the stationary force-line of  $L_1$ . Now the limbs  $L_1, L_2, L_3$  form a 3-legged equilibrium posture, and the spider can lift the limb  $L_4$ . Note that in both modes of locomotion the spider is continuously immobile with respect to the tunnel walls. During limb lifting the spider is immobilized by surface curvature effects ( $m_{q_0}^1 > 0$  and  $m_{q_0}^2 = 0$ ). During limb repositioning the spider is immobilized by first-order effects ( $m_{q_0}^1 = 0$ ). Immobilization implies that the naturally occurring compliance at the contacts stabilizes the mechanism against any external disturbances (Rimon and Burdick, 1998b). Hence, if the inertial forces due to moving parts of the spider are kept small, the reaction forces at the contacts would automatically compensate for the inertial forces, resulting in a *locally stable locomotion* of the mechanism.

The planning of the spider's motion using the two modes of locomotion involves other issues not considered here. First, we must select a sequence of foothold positions which leads the spider to its goal, such that each new foothold is reachable from the spider's current position. Second, we must generate a collision-free trajectory which moves the spider between successive footholds according to the above two modes of locomotion. A motion planner that performs all these tasks will be described in a future paper. We also note a related work by Madhani and Dubowsky on planning the motion of spider-like mechanisms (Madhani and Dubowsky, 1997). However, they use friction effects while we consider motion that does not rely on friction.

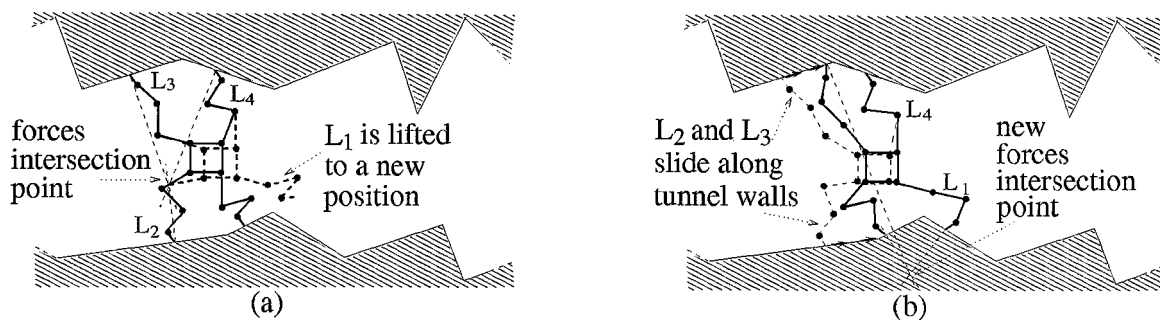


Figure 9. The two motion phases of the spider. (a) Limb lifting of  $L_1$ . (b) Limb repositioning in preparation for the lifting of  $L_4$ .

## 5. An Immobilization-Based Control for the Spider

In this section we describe a control methodology for executing the motion phases described above. First we give an overview of the method, then discuss its technical details.

### 5.1. Overview of the Control Approach

The spider has four limbs each having four actuated degrees of freedom. The central base of the spider possesses additional three degrees of freedom. The spider thus has a total of *nineteen* degrees of freedom, of which only *sixteen* are actuated. However, the spider is *not* an underactuated system. Consider for simplicity the limb-lifting mode of locomotion. During this motion phase the spider braces itself with three limbs while the fourth limb moves to a new position. The contacting limbs introduce three scalar constraints which effectively force the spider to move in a 16-dimensional manifold, denoted  $\mathcal{N}$ , which lies in the 19-dimensional configuration space of the spider. The control problem is how to transfer the torques generated by the spider's sixteen actuators to the 16-dimensional manifold  $\mathcal{N}$ . In particular, we wish to induce forces and torques on the spider's central base in order to bring it to a desired position and orientation.

Our control approach relies on the immobilization of the spider by the tunnel walls. As long as the footpads maintain an immobilizing posture with respect to the environment, the reaction forces generated by the natural compliance present at the contacts will tend to stabilize the mechanism as a single rigid body. See Refs. Howard and Kumar (1996) and Lin et al. (1997) for a Hertz model analysis of this process. Our control approach thus consists of the following active and passive components. The active component is implemented by servoing the spider's joint actuators in a way which keeps the contacting footpads fixed relative to each other. From the perspective of the tunnel walls, the mechanism consequently behaves as a single rigid body immobilized by the tunnel walls. Note, however, that we are still free to guide the spider's free limb and central base along any desired trajectory, as long as the contacting footpads remain fixed relative to each other. The passive component of the control relies on the reaction forces generated by the tunnel walls. These forces act through the footpads and tend to keep the spider as a single rigid body at the same position and

orientation. In other words, the tunnel walls will automatically cancel all sufficiently small inertial forces generated by the moving parts of the spider. When the free limb reaches its destination, the associated inertial forces vanish, and the spider's contacting footpads will settle at their precise original location.

We note that Pfeiffer et al. (2000) have suggested an alternative control approach for spider-like robots which also relies on compliance at the contacts. However, their objective is to control the forces at the contacts rather than the configuration of the spider. Controlling the contact forces seems harder than merely maintaining the contacts at a desired position, since the contact forces depend on the material properties of the footpads and the environment, and these properties may vary widely in any practical scenario.

### 5.2. Details of the Control Law

First let us introduce some notation. Let  $q_i \in \mathbb{R}^4$  denote the  $i$ th limb joint vector, and let  $\bar{q} = (q_1, q_2, q_3, q_4) \in \mathbb{R}^{16}$  denote the entire spider joint vector. Let  $\tau_i \in \mathbb{R}^{16}$  denote the  $i$ th limb torque vector, and let  $\tau \in \mathbb{R}^{16}$  denote the entire spider joint torques. The configuration of the spider's central base (position and orientation) is denoted by the vector  $q_b \in \mathbb{R}^3$ , and the entire configuration of the spider is denoted by the vector  $q = (q_b, \bar{q}) \in \mathbb{R}^{19}$ . The contact point between the  $i$ th limb and the environment, described in a fixed reference frame, is denoted  $x_i \in \mathbb{R}^2$ . The point  $x_i$  depends on the configuration of the central base and the  $i$ th limb, and we write this dependency as  $x_i(q_b, q_i)$ . The contact force applied by the environment to the  $i$ th footpad is denoted by  $F_i \in \mathbb{R}^2$ . Note that when  $F_i = 0$  the  $i$ th limb is not contacting the environment. Each contact force  $F_i$  induces a wrench (i.e. force and torque) on the central base, and torques on the joints of the  $i$ th limb. The vector  $w_i \in \mathbb{R}^{19}$  denotes these wrench and torques, with the understanding that  $w_i$  has zeroes at the components corresponding to the other limbs. The net wrench and torques due to all contact forces is the sum  $\sum_{i=1}^4 w_i$ .

In general, each vector  $w_i$  is given by the formula  $w_i = Dx_i(q_b, q_i)^T F_i$ , where  $Dx_i(q_b, q_i)$  is the  $2 \times 19$  Jacobian matrix of  $x_i(q_b, q_i)$ . (Here again,  $w_i$  has zeroes in the components corresponding to the other limbs.) In our case, we assume that the contact forces are generated by compliance effects at the contacts. These compliance effects are governed by an *elastic potential energy function* (Rimon and Burdick, 1998), whose value depends on the amount of penetration of

the  $i$ th footpad into the tunnel walls. Intuitively, any configuration  $q = (q_b, \bar{q})$  of the spider determines a particular penetration of the  $i$ th limb into the tunnel wall, and this penetration determines a particular value for the elastic potential energy at the  $i$ th contact. We denote by  $\Pi_i(q)$  the elastic potential at the  $i$ th contact, and note that  $\Pi_i$  is non-negative and vanishes when the  $i$ th footpad is disjoint from the tunnel walls. The torques-and-wrench vector  $w_i$  due to the elastic potential energy  $\Pi_i$  is given by  $w_i = Dx_i(q_b, q_i)^T F_i = -\nabla \Pi_i(q)$ .

We can now write the dynamical equation of the spider<sup>3</sup>:

$$M(q)\ddot{q} + B(q, \dot{q}) = \begin{pmatrix} \vec{0} \\ \tau \end{pmatrix} - \sum_{i=1}^4 \nabla \Pi_i(q), \quad (5)$$

where  $M(q)$  is the  $19 \times 19$  inertia matrix of the spider, and  $B(q, \dot{q})$  is the term corresponding to centrifugal and Coriolis forces acting along the spider's nineteen degrees of freedom. The vector  $\vec{0}$  appearing in (5) is a vector of three zeroes, corresponding to the unactuated degrees of freedom of the spider's central base. As discussed above, our control approach consists of servoing the spider's joints in a way which keeps the contacting footpad fixed relative to each other. At each control step, a high-level motion planner provides the controller with a desired collision-free configuration for the spider, denoted  $q^* = (q_b^*, \bar{q}^*)$ . The motion planner additionally ensures that at  $\bar{q} = \bar{q}^*$  the three contacting footpads are at their original bracing position with respect to each other. We use the following simple PD law to servo the spider's joints about the desired joint values  $\bar{q}^*$ :

$$\tau(t) = -K_p(\bar{q}(t) - \bar{q}^*) - K_d\dot{\bar{q}}(t), \quad (6)$$

where the proportional and damping matrices  $K_p$  and  $K_d$  are  $16 \times 16$  positive definite matrices. A choice of diagonal matrices  $K_p$  and  $K_d$  gives a *decentralized* control of the spider, where every joint controller need only know its own state.

A proof of stability of the control law (6) is sketched in the appendix. We have implemented a dynamic simulation of the closed-loop spider system, using the Hertz contact model for the compliance at the contacts. The simulations show excellent convergence properties of the control method in both modes of locomotion of the spider. For example, using material properties of Aluminum at the contacts, the spider converges to a desired limb position within 5 cm range in less than 0.05 seconds. Using material properties of Rubber at the contacts, the spider converges to a desired limb position within 5 cm range in a slower time of less than 0.5 seconds. The simulation results as well as full locomotion experiments will be discussed in a future paper that will focus on the immobilization-based controller. The future paper will also provide a procedure for selecting the matrices  $K_p$  and  $K_d$  in (6) according to desired performance criteria.

## 6. Experiments with the Spider Robot

The spider robot has been built and snapshots of the spider bracing against tunnel walls are shown in Fig. 10. The actuators and sensors used by the mechanism are the standard ones. Specifically, the spider is actuated by small Maxon DC servo-motors each having an optical encoder, and the position and orientation of the central-base is measured by a CCD camera mounted above the experiment. In this section we describe experiments that verify the robustness of the mechanism's

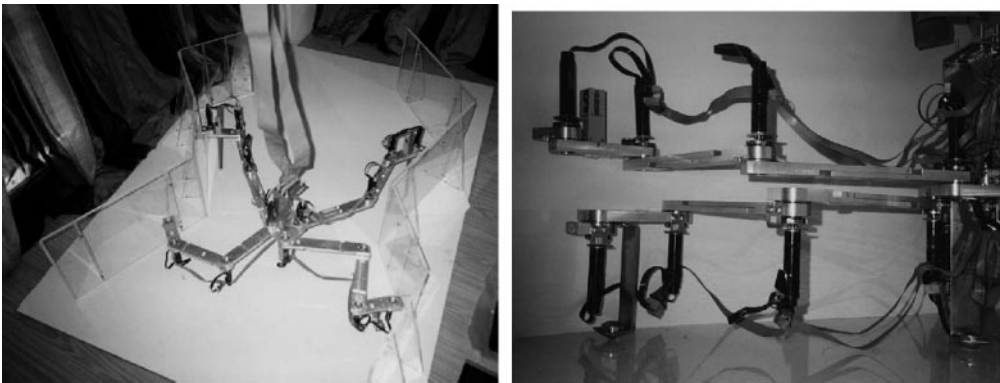


Figure 10. Snapshots showing top and side views of the spider bracing against tunnel walls.

equilibrium postures with respect to small footpad placement errors.

First, consider 3-legged equilibrium postures. These postures are particularly sensitive to footpad placement errors, since arbitrarily small placement errors would yield force-lines that do not intersect at a common point as required for equilibrium. We now describe two approaches that compensate for such errors. The first approach replaces the footpads that maintain a single contact point with the environment with footpads that maintain multiple contacts with the environment. For example, the roller-bearing footpad depicted in Fig. 8(b) maintains two frictionless contacts with the tunnel walls. Using this footpad design, the two contacts of each footpad determine a strip of contact normals. It can be verified that as long as the strips of the individual footpads have a common intersection, the associated posture is an immobilizing equilibrium posture. Hence if we plan a nominal equilibrium posture for the center lines of the three strips, each footpad may deviate by half-width of a strip without harming the equilibrium or its stability.

The second approach exploits friction, which is present even in a small amount at the contacts. Friction effects induce a neighborhood of footpad placements about the nominal frictionless placement which hold the mechanism in a stable 3-legged equilibrium.<sup>4</sup> To see this fact, consider the frictionless 3-legged equilibrium posture shown in Fig. 11. The force-lines intersect at  $p$ , the  $i$ th contact force magnitude is  $F_i$ , and the distance between the  $i$ th contact point and  $p$  is  $\rho_i$ . Suppose that one of the footpads, with index  $i_0$ , is placed at a distance  $\delta$  from its nominal position along the tunnel wall. Then the torque about  $p$  induced by a placement

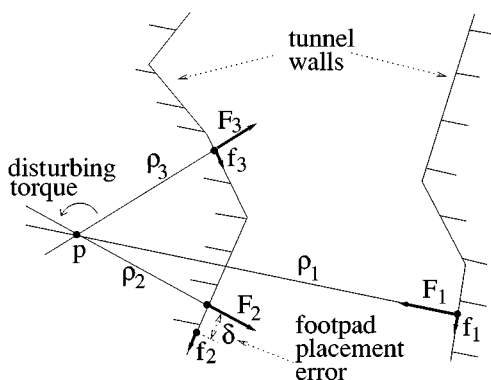


Figure 11. A 3-legged immobile posture with an error  $\delta$  in the placement of the second footpad (only the contact points are shown).

error  $\delta$  is:  $\eta = \delta F_{i_0}$ . If we assume frictional contacts, these contacts generate tangential forces that compensate for the torque  $\eta$ . Let  $f_i$  denote the magnitude of the tangential frictional force at the  $i$ th contact. Then the frictional torque about  $p$  is  $\rho_i f_i$ , and for equilibrium of torques about  $p$  we must have  $\eta = \sum_{i=1}^3 \rho_i f_i$ . Letting  $\mu$  be the coefficient of friction,  $f_i \leq \mu F_i$  according to the Coulomb friction law. Substituting the inequality  $f_i \leq \mu F_i$  in the equilibrium condition gives:  $\delta \leq (\mu \sum_{i=1}^3 \rho_i F_i) / F_{i_0}$ . Any footpad placement error  $\delta$  satisfying this inequality would be compensated by friction effects and still generate a stable equilibrium posture. The inequality also implies that a small amount of friction suffices to compensate for reasonable footpad placement errors. Since the contact forces have approximately the same magnitude, we obtain the approximate equilibrium condition  $\delta \leq \mu \sum_{i=1}^3 \rho_i$ . Interpreting this inequality as a condition on the coefficient of friction  $\mu$ , we obtain  $\mu \geq \delta / \sum_{i=1}^3 \rho_i$ . However,  $\delta$  is in the range of a few millimeters while  $\sum_{i=1}^3 \rho_i$  is in the range of tens of centimeters. Substituting  $\delta = 10$  mm and  $\sum_{i=1}^3 \rho_i = 100$  cm gives that a small coefficient of friction  $\mu = 0.01$  already suffices to compensate for reasonable footpad placement errors.

We have experimentally tested the friction-based error compensation approach on the 3-legged equilibrium posture depicted in Fig. 11. In our experiment the footpads are made of Aluminum while the tunnel walls are made of thick Perspex plates. The coefficient of friction between the footpads and tunnel walls was originally  $\mu = 0.3$ , and this coefficient was reduced to  $\mu = 0.1$  by lubricating the tunnel walls with Teflon spray. We initially established a 3-legged immobile frictionless equilibrium posture, whose contact force magnitudes are  $F_1 = 272$  gr,  $F_2 = 214$  gr, and  $F_3 = 86$  gr. The distances of the contact points from  $p$  are  $\rho_1 = 132.6$  cm,  $\rho_2 = 50.3$  cm, and  $\rho_3 = 53.4$  cm. Substituting this data using  $i_0 = 2$  to designate a placement error in the second footpad, we obtain the conservative bound  $\delta \leq (\mu \rho_1 F_1) / F_2 = (0.1 \cdot 132.6 \cdot 272) / 214 = 16.8$  cm. In our experiment, we varied the placement error of the second footpad by increments of 5 mm, and obtained stable equilibrium postures up to a distance of 55 mm from the nominal footpad position. (Larger placement errors were hard to verify due to kinematic reachability constraints of the mechanism.) Since practical footpad placement errors are expected to be in the range of a few millimeters, a small amount of friction would suffice to maintain stability in the presence of such errors.

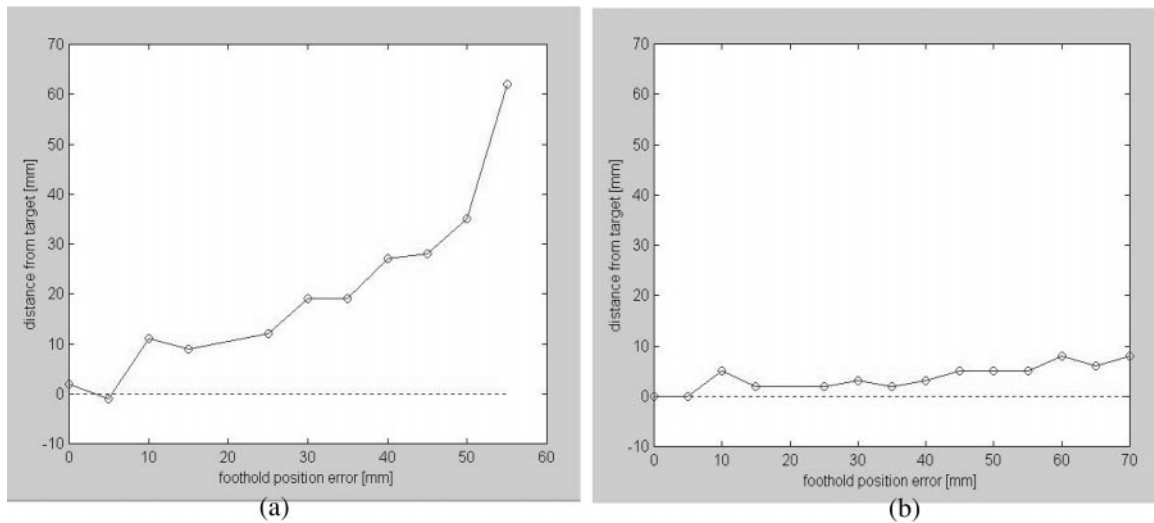


Figure 12. Central-base position error at the end of a straight-line motion due to footpad placement errors. (a) Position error during 3-legged immobilization. (b) Position error during 4-legged immobilization.

Our next experiment measures the accuracy of the spider's motion during 3-legged immobilization. The 3-legged posture has the geometry depicted in Fig. 11. In this experiment, too, we have lubricated the tunnel walls to achieve a  $\mu = 0.1$  coefficient of friction. The spider in this experiment is bracing against the tunnel walls while its central-base moves 70 mm along the tunnel's central axis. The motion is executed using the immobilization-based controller described above, with one intermediate point specified at a distance of 35 mm along the tunnel's central axis. The accuracy of the motion is measured by the Euclidean distance of the central-base position at the end of motion from its desired final position. The graph in Fig. 12(a) depicts the central-base position error as a function of a footpad placement error. Using placement error increments of 5 mm, it can be seen that the central-base motion accuracy remains within a few millimeters for footpad placement errors of up to  $\delta = 10$  mm. Beyond this value, inertial forces generated during the spider's motion dominate the small frictional forces at the contacts. These inertial forces cause local slips at the contacts, with a resulting large error in the central-base final position.

Our final experiment measures the central-base motion accuracy during 4-legged immobilization. In contrast with 3-legged immobilization, 4-legged equilibrium postures are *inherently robust* with respect to footpad placement errors. Once a nominal 4-legged

equilibrium posture is established, all nearby footpad placements are automatically equilibrium postures, even in a frictionless environment. Moreover, almost all 4-legged equilibrium postures are immobile. Hence, we expect a significantly better motion accuracy during 4-legged immobilization. The graph shown in Fig. 12(b) indicates the central-base position error at the end of a motion toward a target located at a distance of 55 mm along the tunnel's central axis. As above, the motion is generated by the immobilization-based controller with one intermediate point specified at a distance of 27.5 mm along the tunnel's central axis. Using placement error increments of 5 mm, it can be seen that now the motion accuracy decreases more slowly, with an of a few millimeters for footpad placement errors of up to  $\delta = 70$  mm.

The experiments in both types of immobilization show robustness with respect to footpad placement errors in the range of a few millimeters for 3-legged immobilization and a few centimeters for 4-legged immobilization. However, robustness during 3-legged immobilization is achieved by either using a multiple-contact frictionless footpad, or by exploiting friction effects at the contacts. Both of these approaches deviate from our formal assumptions of single-contact frictionless footpads. Indeed, we discuss in the concluding section our current research which is concerned with the inclusion of friction effects into the locomotion.

## 7. Concluding Discussion

We described the design of a spider-like robot capable of quasistatic locomotion in two-dimensional tunnel environments. We have made a worst-case assumption of slippery tunnel walls. Under this assumption, the immobilization theory dictated that the smallest number of limbs such a mechanism can have is *four*. The theory also dictated the footpads' curvature required for stable locomotion of the robot. Other key parameters, such as the dimension and number of degrees of freedom of each limb, were dictated by the class of tunnel geometries. We also described a two-phased locomotion strategy for the spider robot under the assumption of slippery tunnel walls. In the first phase the spider lifts a limb to a new position while bracing with three limbs against the tunnel walls. In the second phase the spider contacts the environment with all four limbs while adjusting its contacts along the tunnel walls in preparation for the lifting of a new limb. Finally, we described a decentralized control method for executing the two motion phases, whereby immobilization effects are used to induce forces and torques on the spider's central base. The spider has been built, and experiments verifying its robustness with respect to footpad placement errors were described.

Future extensions of this work will focus on the inclusion of *friction and gravity* into the locomotion. The inclusion of friction will allow the spider to move in tunnels of a particular simple geometry such as two parallel lines, as is often the case in man-made environments. However, the inclusion of friction raises several technical challenges. The first challenge is to efficiently estimate the amount of friction in a particular foothold area. This problem is especially acute in unstructured tunnel environments, where surface material properties and environmental conditions may vary widely during locomotion. A second challenge is how to guarantee adequate disturbance rejection with frictional contacts, given the bounded-torque capability of the spider's actuators. A third challenge is the need to develop a method for controlling the spider's contact forces with the environment, as to prevent slip at the contacts (Pfeiffer et al., 2000). Note that in our immobilization-based approach the controller has the simpler task of merely maintaining the footpads at a desired position.

In order to include gravity in the experiments, we plan to tilt the horizontal tunnel-plane by  $45^\circ$ , so that gravity would act in the plane of the two-dimensional

tunnel. As long as the spider braces itself against the tunnel walls during locomotion, the inclusion of gravity should require only minor modifications to the spider's horizontal motion-and-control algorithms. Such a quasistatic bracing motion can provide the spider with significant payload and disturbance-rejection capabilities. However, it is also possible to seek a design which employs the smallest number of limbs required for stable locomotion in a gravitational field. It seems that gravity can be regarded as a "virtual leg" which presses on the mechanism's center of gravity along a fixed direction. Although such a leg is less versatile than a mechanical leg, by suitably adjusting the mechanism's center of mass, a legged robot should be able to stably move in two-dimensional gravitational environments using only *three* legs (Dubowsky et al., 1999). Such a stable motion seems feasible even over slippery terrains, provided that the terrain contains many footholds of varying orientations, as is often the case in unstructured terrains. The validation of this hypothesis is a major challenge which we plan to explore in future work.

## Appendix

### A. Sketch of Proof of Stability

In this appendix we sketch the stability proof for the closed-loop spider system under the control law (6). For simplicity, we assume that at  $q = q^*$  the spider contacts the tunnel walls, but does not actually penetrate these walls. It follows that the total elastic energy associated with the contacts,  $\Pi(q) = \sum_{i=1}^4 \Pi(q_i, q_b)$ , vanishes at  $q = q^*$ . Consider now the following Lyapunov function candidate for the closed-loop system:

$$V(q) = \frac{1}{2} \dot{q}^T M(q) \dot{q} + \Pi(q) + \Phi(\bar{q}) \quad \text{where}$$

$$\Phi(\bar{q}) = \frac{1}{2} (\bar{q} - \bar{q}^*)^T K_p (\bar{q} - \bar{q}^*).$$

The first term in  $V$  is the kinetic energy of the spider; the second term is the elastic energy associated with the contacts; and the third term is the potential energy associated with the proportional term in the control law. We note that more sophisticated expressions for  $\Phi(q)$  can be used without affecting the stability result, including expressions that account for obstacle avoidance.

The point  $q = q^*$  with zero velocity is a *local minimum* of  $V$  as required for a Lyapunov function, for

the following reasons. First, the three terms in  $V$  are non-negative and vanish at  $(q, \dot{q}) = (q^*, 0)$ . Moreover, for any deviation from  $(q, \dot{q}) = (q^*, 0)$  one of these terms becomes strictly positive. Intuitively,  $\Pi$  becomes strictly positive for any motion of the spider as a single rigid body, since the spider is immobilized by the tunnel walls at  $q = q^*$ . Similarly, any change of joint values with respect to  $\bar{q} = \bar{q}^*$  will cause the quadratic term  $\Phi(\bar{q})$  to become strictly positive. We can now interpret the closed-loop system as being governed by a combined potential energy of the form  $U(q) = \Pi(q) + \Phi(q)$ , and invoke a standard result concerning the stability of mechanical systems governed by a potential energy function (Koditschek, 1989; Thompson and Tait, 1886). According to this result, *the local minima of  $U$ , with zero velocity, of a damped mechanical system are local attractors of its flow*. Since damping is introduced into the closed-loop system by the matrix  $K_d$  in (6), the closed-loop spider system is locally asymptotically stable around the desired configuration  $q^*$  with zero velocity.

## Notes

1. The scalar multiplying  $n_i(q_0)$  is positive since the contact forces can only push on  $\mathcal{B}$ .
2. In general, the collection of 3-contact planar equilibrium grasps or postures is a two-dimensional set (Stappen et al., 1999).
3. The gradient of  $\Pi_i$  is differentiable, hence existence and uniqueness of solutions to (5) is assured.
4. Frictional equilibrium postures are force-closure stable, which is a weaker form of stability than frictionless immobilization.

## References

- Boissonnat, J.-D., Devillers, O., Donati, L., and Preparata, F.P. 1992. Motion planning for spider robots. In *IEEE Int. Conf. on Robotics and Automation*, pp. 2321–2326.
- Chirikjian, G.S. and Burdick, J.W. 1993. Design and experiments with a 30 degree-of-freedom hyper-redundant robot. In *IEEE Int. Conf. on Robotics and Automation*, Vol. 3, pp. 113–117.
- Czyzowicz, J., Stojmenovic, I., and Urrutia, J. 1991. Immobilizing a polytope. *Lecture Notes in Computer Science*, Vol. 519, Springer-Verlag, Berlin, pp. 214–227.
- Dubowsky, S., Sunada, C., and Marvoidis, C. 1999. Coordinated motion and force control of multi-limbed robotic systems. *Autonomous Robots*, 6:7–20.
- Gray, J. 1993. *How Animals Move*. Cambridge University Press: Cambridge, London, 1953.
- Hirose, S. and Kunieda, O. 1991. Generalized standard foot trajectory for a quadruped walking vehicle. *Int. J. Robotics Research*, 10(1):2–13.
- Hirose, S. and Morishima, A. 1990. Design and control of a mobile robot with an articulated body. *Int. J. Robotics Research*, 9(2): 99–114.
- Howard, W.S. and Kumar, V. 1996. On the stability of grasped objects. *IEEE Transactions on Robotics and Automation*, 12(6): 904–917.
- Koditschek, D.E. 1989. The application of total energy as a Lyapunov function for mechanical control systems. In *Control Theory and Multibody Systems*, AMS Series in Contemporary Mathematics, Vol. 97, J. Marsden, Krishnaprasad, and J. Simo (Eds.). AMS: Providence, RI, pp. 131–158.
- Lin, Q., Burdick, J.M., and Rimon, E. 1997. Computation and analysis of compliance in grasping and fixturing. In *IEEE Int. Conf. on Robotics and Automation*, pp. 93–99.
- Madhani, A. and Dubowsky, S. 1992. Motion planning of mobile multi-limb robotic systems subject to force and friction constraints. In *IEEE Int. Conf. on Robotics and Automation*, pp. 233–239.
- Madhani, A. and Dubowsky, S. 1997. The force workspace: A tool for the design and motion planning of multi-limb robotic systems. *ASME Journal of Mechanical Design*, 119(2):218–225.
- Markenscoff, X., Ni, L., and Papadimitriou, C.H. 1990. The geometry of grasping. *Int. Journal Robotics Research*, 9(1):61–74.
- Marhefka, D.W. and Orin, D.E. 1997. Gait planning for energy efficiency in walking machines. In *IEEE Int. Conf. on Robotics and Automation*, pp. 474–480.
- McGeer, T. 1989. Powered flights, child's play, silly wheels and walking machines. In *IEEE Int. Conf. on Robotics and Automation*, pp. 1592–1597.
- Nagakubo, A. and Hirose, S. 1994. Walking and running of the quadruped wall-climbing robot. In *IEEE Int. Conference on Robotics and Automation*, pp. 1005–1012.
- Neubauer, W. 1993. Locomotion with articulated legs in pipes or ducts. In *Int. Conf. on Intelligent Autonomous Systems*, pp. 64–71.
- Neubauer, W. 1994. Spider-like robot that climbs vertically in ducts or pipes. In *IEEE/RSJ/GI International Conference on Intelligent Robots and Systems*, Vol. 2, pp. 1178–1185.
- Pfeiffer, F., Chernousko, F., Bolotnik, N., Robmann, T., and Kostin, G. 2000. Tube-crawling robot: Modeling and optimization. *IEEE Trans. on Robotics and Automation*. Submitted for publication.
- Reuleaux, F. 1963. *The Kinematics of Machinery*. Macmillan 1876, republished by Dover: New York.
- Rimon, E. and Burdick, J.W. 1995. New bounds on the number of frictionless fingers required to immobilize planar objects. *J. Robotic Systems*, 12(6):433–451.
- Rimon, E. and Burdick, J.W. 1998a. Mobility of bodies in contact—I: A 2nd order mobility index for multiple-finger grasps. *IEEE Trans. on Robotics and Automation*, 14(5):696–708.
- Rimon, E. and Burdick, J.W. 1998b. Mobility of bodies in contact—II: How forces are generated by curvature effects. *IEEE Trans. on Robotics and Automation*, 14(5):709–717.
- Rimon, E., Shoval, S., and Shapiro, A. 1999. Design of a quadruped robot for motion with quasistatic force constraints. Technical report, Dept. of Mechanical Engineering, Technion.
- Roassmann, T. and Pfeiffer, F. 1996. Control and design of a pipe crawling robot. In *13th World Congress of Automatic Control*, San Francisco, USA.
- Stone, T.J., Cook, D.S., and Luk, B.L. 1995. Robug III—The design of an eight legged teleoperated walking and climbing robot for disordered hazardous environments. *Mechanical Incorporated Engineer*, 7(2):37–41.

Shan, Y. and Koren, Y. 1993. Design and motion planning of a mechanical snake. *IEEE Trans. on Systems Man and Cybernetics*, 23(4):1091–1100.

Thompson, Sir W. and Tait, P.G. 1886. *Treatise on Natural Philosophy*. University of Cambridge Press: Cambridge.

Van Der Stappen, A.F., Wentink, C., and Overmars, M.H. 1999. Computing form closure configurations. In *IEEE Int. Conf. on Robotics and Automation*, pp. 1837–1842.

van der Doel, K. and Pai, D.K. 1997. Performance measures for locomotion robots. *J. of Robotic Systems*, 14(2):135–147.

**Elon Rimon** received the B.Sc. degree in computer engineering from the Technion, Israel Institute of Technology, Haifa, in 1985 and the Ph.D. degree in electrical engineering from Yale University, New Haven, CT, in 1990. He was appointed Lecturer of Mechanical Engineering at the Technion in 1994, where he is presently a Senior Lecturer. His interests geometrical reasoning in robotics, sensor based motion planning, and locomotion of multi-limbed machines.

**Shraga Shoval** received B.Sc. and M.Sc. in mechanical engineering at the Technion—Israel Institute of Technology in 1985 and 1987. Between 1987 and 1990 worked as a scientist at the CSIRO—Division of Manufacturing Technologies, Sydney, Australia. In 1994 completed his Ph.D. studies at the department of Mechanical Engineering at the University of Michigan, Ann-Arbor. Was a member of the U of M winning team for the first Mobile Robot competition organized by the American Association of Artificial Intelligence (AAAI). Between 1994 and 1999 he worked as a Research Fellow and lecturer at the faculty of Industrial Engineering and Management at the Technion. Currently he is the head of the department of Industrial Engineering & Management at the J&S Academic college in Ariel.

**Amir Shapiro** received the B.Sc. and M.Sc. degrees in Mechanical Engineering from the Technion, Israel Institute of Technology, Haifa, in 1997 and 2000. He is presently a Ph.D. candidate in the Department of Mechanical Engineering at the Technion, Israel Institute of Technology. His interests include mechanical design, control, and quasistatic locomotion of multi-limbed machines.